Infrared radiation measurements of a recombining CO2 plasma at atmospheric pressure

Corentin H C Grimaldi, Sean D Mcguire, Augustin Tibère-Inglesse, Christophe O Laux

Infrared radiation measurements of a recombining CO_2 plasma at atmospheric pressure

Corentin H. C. Grimaldi[1], Sean D. McGuire[2], Augustin Tibère-Inglesse[3] and Christophe O. Laux[4]

Laboratoire EM2C, CNRS UPR288, CentraleSupélec, Université Paris-Saclay, 3 rue Joliot Curie, 91190 Gif-sur-Yvette, France

High resolution infrared emission measurements are performed on a high temperature CO_2/Ar plasma. A 50 kW ICP torch was used to produce an atmospheric pressure CO_2/Ar plasma jet close to Local Thermodynamic Equilibrium conditions at 6920 K. The emission measurements on this plasma jet were made between 0.9 and 5.6 µm. Our goal is to study the emission and verify that this emission is correctly modeled by the line-by-line radiation code SPECAIR. The measured spectra, calibrated in absolute intensity, are therefore compared with calculations done using SPECAIR. The absolute intensities of several atomic lines are used to measure the temperature of the plasma. This method gives the temperature quite accurately within the central hot portion of the plasma jet. We find that the molecular emission coming from this portion of the jet matches well the SPECAIR predictions. Large portions of the observed CO_2 and CO molecular emission are emitted from the colder regions of the jet where the atomic lines are not sufficiently strong to provide a measure of temperature. In this paper, these colder portions of the molecular band emission are not compared with SPECAIR predictions.

I.Introduction

The entry of a capsule into the atmosphere of a planet or a satellite occurs at hypersonic velocities. The resulting shock wave that forms in front of the vehicle heats the surrounding gas and forms a plasma in the post-shock region. The study of the resulting convective and radiative heat fluxes to the capsule surface is critical for the design of the thermal protective system [1]. For Mars entry scenarios, where the CO_2 represents 96% of the atmosphere [2], the radiative heat flux to the afterbody suffers from large uncertainties up to 260% [3]. The rapid hydrodynamic expansion of the plasma into the afterbody results in rapid cooling, chemical recombination and a departure from equilibrium [4]. This chemical non-equilibrium and the associated radiation are still not accurately modeled, and our goal is to provide experimental data for model validation as part of an effort to help reduce this uncertainty. Our experiments focus on a fundamental study of the recombination dynamics of CO_2 plasmas – specifically, the relevant recombination kinetics [5]. For these experiments, the plasma is first created by an inductively coupled plasma torch facility. The plasma is then passed through a water-cooled tube at high speed to force rapid cooling and chemical recombination. Optical and laser diagnostics then allow us to track the recombination and cooling that results [6], [7].

The infrared spectral region is of interest because it provides direct measurements of CO and CO_2 ground state densities and rovibrational population distributions [8]. This work represents a continuation of the work begun last year [9] looking at UV, visible and near IR emission spectra from a CO_2/Ar plasma. This paper presents our first IR measurements obtained between 0.9 and 5.6 µm. These measurements are done directly at the exit of the inductively

[1] Ph.D. Student, Laboratoire EM2C, CNRS UPR288, CentraleSupélec, Université Paris Saclay.
[2] Assistant Professor, Laboratoire EM2C, CNRS UPR288, CentraleSupélec, Université Paris Saclay, AIAA Member.
[3] Post doctorate, Laboratoire EM2C, CNRS UPR288, CentraleSupélec, Université Paris Saclay.
[4] Professor, Laboratoire EM2C, CNRS UPR288, CentraleSupélec, Université Paris Saclay, AIAA Associate Fellow.

coupled plasma torch (ICP) which represents the tube inlet. Our goal is to study the highly resolved emission spectrum that we measure and to verify that this emission is correctly modeled by the line-by-line radiation code SPECAIR. Our future work will then build upon this and look at IR spectra for test cases where the water-cooled tube is used to force cooling and chemical recombination.

II.Experimental setup

The plasma torch facility at laboratoire EM2C produces atmospheric pressure plasmas at temperatures ranging between 6000 and 9000K depending upon the gas mixture used and the power provided to the plasma. The plasma torch employed is a TAFA Model 66 Inductively Coupled Plasma (ICP) torch powered by a 120kVA radio frequency LEPEL Model T-50-3 power supply that operates at 4MHz and that can deliver up to 50 kW to the plasma. Figure 1 shows a schematic of the experimental ICP torch. More details of the plasma torch facility may be found in several references: [6], [10], [11]. The CO_2/Ar plasma studied here exits the torch through a 1-cm diameter nozzle. All emission measurements were made 0.25 cm downstream of the nozzle exit (i.e. *D/4*, where *D* is the diameter of the nozzle) in a region where the flow is expected to be laminar. The previous inlet conditions used for the UV and visible OES measurements made last year [9] have been changed to address several issues that were encountered when pursuing measurements in the IR region. First, the percentage of CO_2 has been increased to maximize the signal coming from the CO and CO_2 molecular bands. A high fraction of argon, easily ionizable, is still required to provide stable and sustainable operating conditions. The mixture used here is composed of 0.978 g/s (±2%) of carbon dioxide premixed with 2.76 g/s (±2%) of argon. Consequently, the mass fractions of the mixture are, respectively, 26% for CO_2 and 74% for Ar. Furthermore, the ratio between the radial and swirl injection has been modified so that we observe the most symmetric emission profile possible in the IR while maintaining stable operating conditions. For this injection mixture, the best results were obtained when 50% of the mixture was injected via the radial injectors and 50% via the swirl injectors. Increasing the swirl injection tends to increase the symmetry of the plasma jet but also tends to reduce the stability of the torch – our choice represents a compromise between these competing effects. Finally, the plate power has been increased to 60 kW, the maximum for this mixture (note that less power is coupled into the plasma).

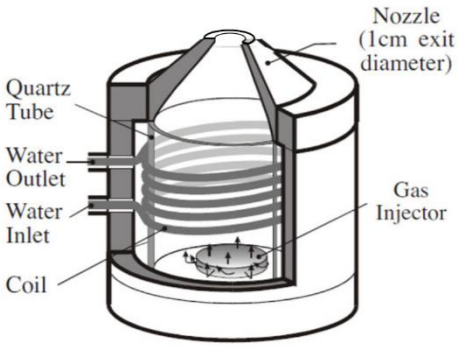

Figure 1. Schematic of ICP torch head, producing a CO_2/Ar plasma close to LTE at atmospheric pressure.

The infrared OES measurements were performed with a 0.75 m focal length spectrometer (Princeton Instruments Acton SpectraPro 2750i) fitted with a 512x640 pixels cryogenically cooled (liquid N2) infrared camera (IRcameras IRC-806). The observed IR background signal strongly drifts with time. To enable us to track and remove this background, a chopper was placed at the entrance to the spectrometer. The background, like the signal coming from the torch, is acquired at the rate of 60 Hz. Two parabolic mirrors (focal length of 20 and 50 cm) were used to collect the signal. Figure 2 show the experimental setup used for the infrared OES measurements. Three different diffraction gratings were used within the spectrometer, a 1200 grooves/mm blazed at 0.75 µm for the 0.9-1.1 µm region, a 600 grooves/mm blazed at 1.6 µm for the 1.1-2.5 µm region and a 300 grooves/mm blazed at 4.0 µm for the 2.5-5.6 µm region. Higher order interferences were rejected by using appropriate long-pass filters with cut-offs at 0.55 µm, 1.05 µm, 1.6 µm, 2.4 µm and 3.6 µm (Melles Griot OG550 and Edmund Optics 68-657, 68-658, 68-659, 68-660 respectively). The combinations of gratings, filters and slit settings over the spectral range are summarized in Table 1.

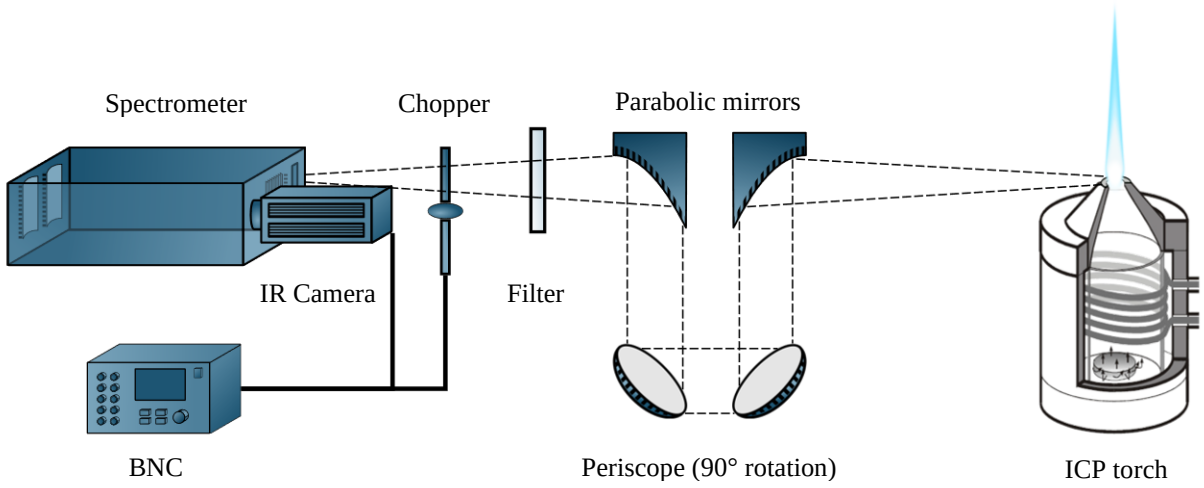

Figure 2. Schematic of the experimental setup used for IR Optical Emission Spectroscopy (OES).

Table 1 Optical element characteristics used for measurements in range 0.9-5.6 µm

Spectral range (µm)	Blaze wavelength λ (µm)	Groove density (gr/mm)	Filter cut-off λ_{min} (µm)	Slit width (µm)
0.9 - 1.1	0.75	1200	0.55	100
1.1 - 2.0	1.6	600	1.05	100
2.0 - 2.5	1.6	600	1.6	100
2.5 - 4.1	4.0	300	2.4	100
4.1 - 5.6	4.0	300	3.6	100

The spectral resolution of the system varies with the wavelength due to the dispersion of the diffraction gratings.Figure 3 Figure 3 shows the evolution of the reciprocal linear dispersion in Å/mm of the three gratings used for the OES measurements over the spectral range of interest [12]. This has important implications for the analysis of the spectra. For example, the Full Width at Half Maximum (FWHM) of the slit function varies over the wavelength range studied. To take this into account in the comparisons with SPECAIR, the slit function was measured at three different wavelengths for each grating used. An interpolation was then used to determine the slit function at a generic wavelength. The FWHM of the slit function was 0.107 nm at 1070 nm, 0.225 nm 1454 nm and 0.442 nm at 5091 nm.

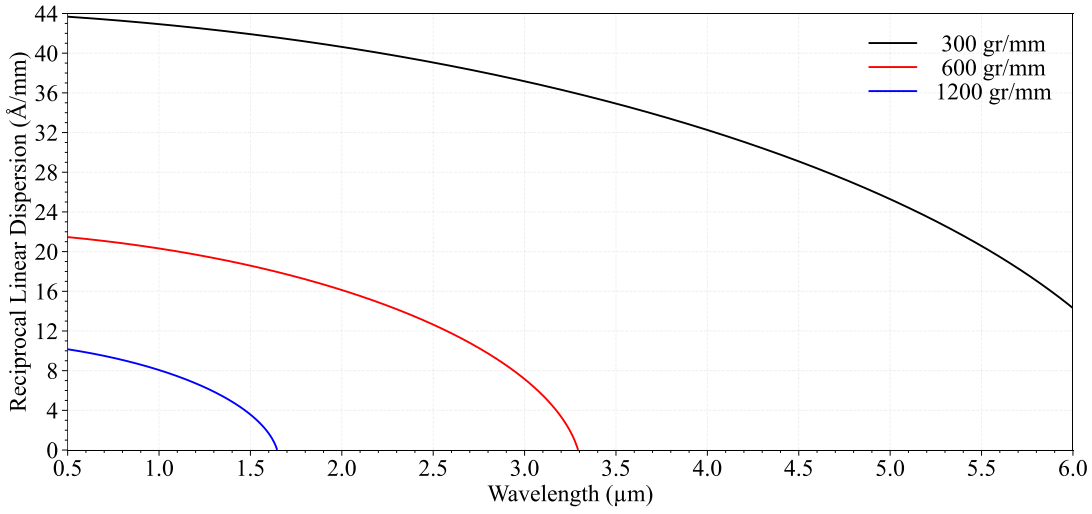

Figure 3. Reciprocal Linear Dispersion of the gratings used for spectral measurements.

III.Calibration in intensity

Absolute calibrations of the spectral intensities were made using a calibrated tungsten lamp traceable to NIST standards (Optronics Laboratory OL 550) equipped with a sapphire window for the IR region. Special attention was paid to accurately calibrate the measurements because cold CO_2 and H_2O present in the optical path absorb the signal at several wavelengths. Figure 4 shows the initial calibration measurements without applying an "absorption correction". The cold CO_2 present in the room is seen to strongly absorb the signal between 4190 and 4370 nm. Absorption from H_2O (due to the humidity of the air) is responsible for the sharp absorption lines observed between 4800 and 5500 nm.

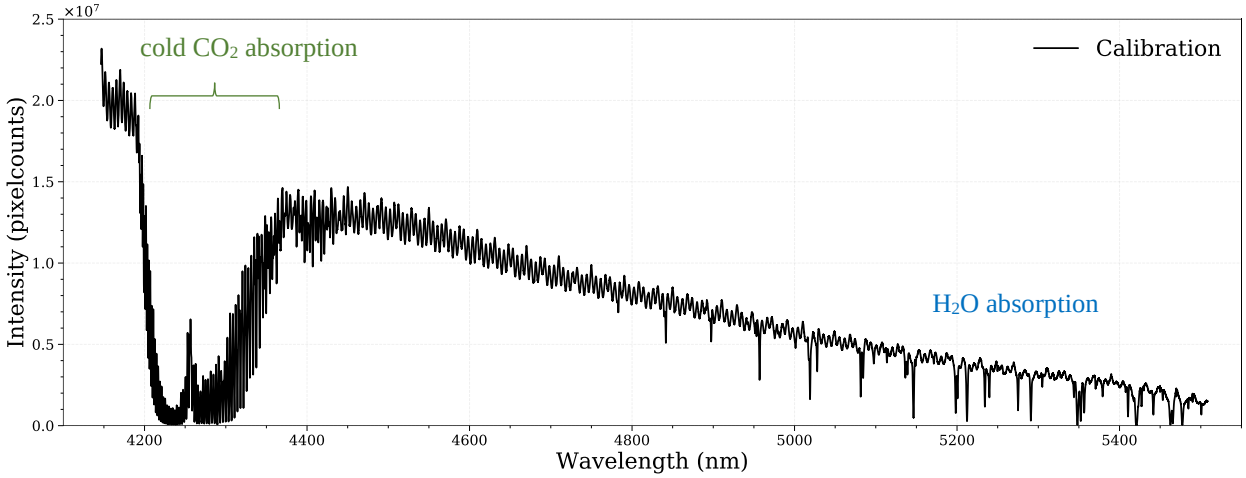

Figure 4. Raw calibration spectrum using the calibrated OL 550 tungsten lamp.

Radiation measurements of the CO_2/Ar plasma using the ICP torch cannot be calibrated using the raw calibration as presented in Figure 4. The absorption from CO_2 and H_2O must first be accounted for as this will impact the torch emission differently. In order to account for this absorption, the transmittance of CO_2 and H_2O is calculated at 293 K and at atmospheric pressure and is then removed from the calibration. The RADIS line-by-line radiation code with the HITEMP database was used for CO_2 and the SPECAIR code for CO [10], [13], [14]. The precise density and path length of CO_2 and H_2O is refined to achieve the best results. This procedure is detailed in Ref. [15] where it was successfully used to measure and model the absorption of OH, NO, and CO_2 at 3400 K.

This method is highly sensitive to the wavelength calibration. Due to this sensitivity, the impact of absorption from cold CO_2 between 4.2 and 4.3 µm in Figure 4 could not be completely removed. We therefore decided to purge 90% of the optical path with N_2, thus decreasing the impact of cold CO_2 and H_2O absorption and permitting an accurate removal from the calibration. Figure 5 to 7 show the calculated CO_2 and H_2O transmittance in green and blue, respectively. The calibration uncorrected for cold gas absorption is shown in black and the absorption-corrected calibration is shown in red. The lack of absorption features in the corrected calibration indicates that these have indeed been accurately removed from the raw calibration spectra. The absorption simulations were made for 46 ppm of CO_2 and 1000 ppm of H_2O (about 4% in relative humidity) over 3.6 m.

Absorption from H_2O due to the humidity of the air, is visible in the calibration measurements across multiple spectral bands. The most impacted regions are shown in Figure 5 and Figure 6 where H_2O strongly absorbs the signal - up to 75% for some lines. This strong absorption is observed despite 90% of the optical path being purged with dry N_2. Between 2.5 and 2.9 µm (Figure 5), the high resolution of the measurements allows to distinguish the fine structure of the absorption lines and to successfully remove them. After 5.0 µm (Figure 6), H_2O is responsible for the sharp and well distinct absorption lines.

Figure 7 shows the calibration after correcting for the absorption coming from cold CO_2 in the room. The purge of the optical path greatly reduced the CO_2 absorption in comparison with Figure 4 where the signal dropped to 0 at its lowest points. Once again, the high resolution of the measurement allows us to see the fine structure of the CO_2 absorption band between 4.2 and 4.35 µm and accurately remove it from the calibration as attests the corrected calibration.

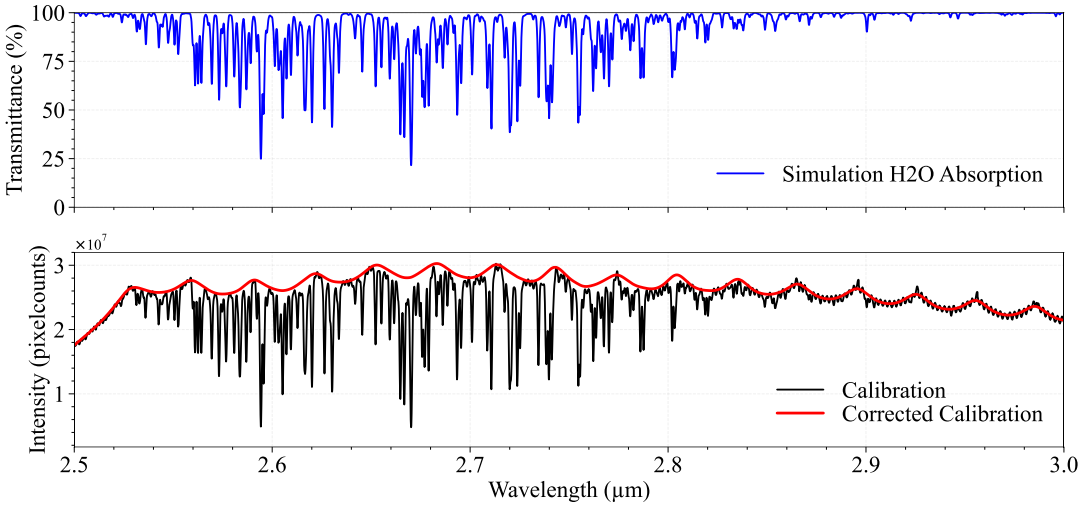

Figure 5. Corrected calibration with H_2O absorption between 2.5 and 3.0 μm.

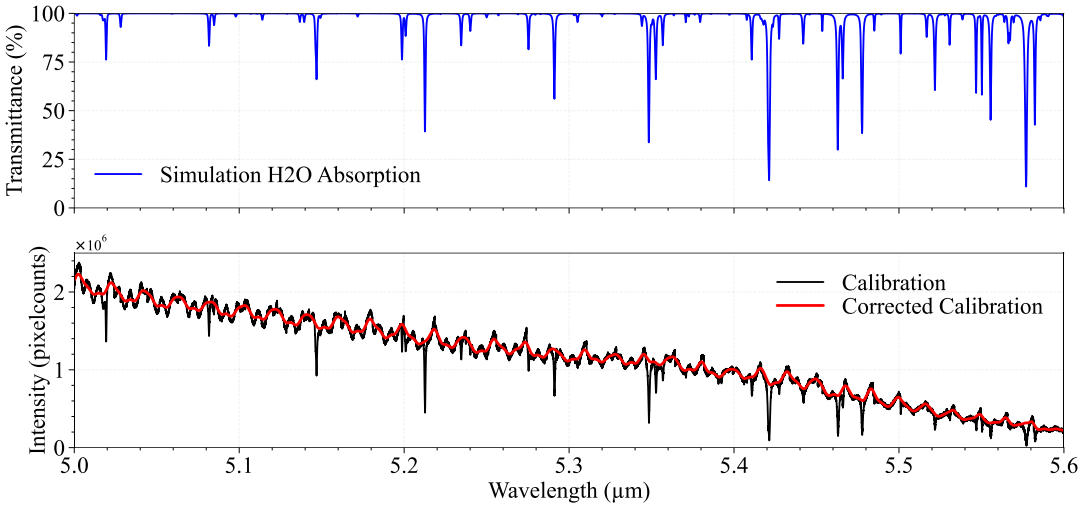

Figure 6. Corrected calibration with H_2O absorption between 5.0 and 5.6 μm.

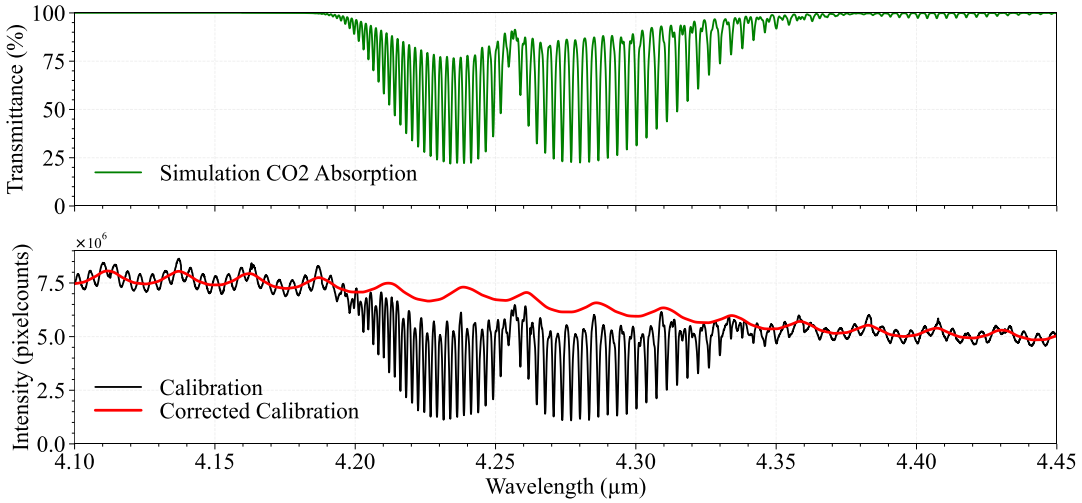

Figure 7. Corrected calibration with CO_2 absorption between 4.1 and 4.45 μm.

Another problem encountered with the measurements was the presence of an "etalon" type interference observed on the camera. This is likely due to an etalon effect occurring within the IR camera. This phenomenon is especially visible in the raw calibration in black on Figure 5 after 2.9 µm and on Figure 7 outside the cold CO_2 absorption band (before 4.2 µm or after 4.35 µm). Note that the interference fringes are visible as a sort of "high frequency" oscillation of the signal. This is not to be confused with the "low frequency" oscillations also observed in the signal which are due to vignetting. The etalon type interferences are not due to absorption. They are also observed in the signal coming from the torch. They are somewhat reproducible, but the interference pattern is highly sensitive to the position of the diffraction grating. For example, if we start at an initial wavelength, then change the grating position to observe another wavelength and finally return back to the initial wavelength, the interference pattern is sufficiently different to make it impossible to remove via calibration. Therefore, we decided to simply smooth these interferences. The resulting amplitude variation, about 5% of the total amplitude, is considered as an uncertainty and is taken into account in the radiation measurements. The corrected calibration is then used to calibrate the spectral intensities of the studied plasma.

IV.OES Measurements

High resolution infrared emission measurements, calibrated in absolute intensity, were performed directly at the exit of the torch from 900 to 5600 nm. Figure 8 to Figure **13** show the absolute intensity measured along the line of sight (LOS) passing through the center of the plasma jet. The absolute intensity of the measured spectral emission is estimated to be accurate to within 10% of the reported amplitudes. Figure 8 to Figure 10 show the OES measurements between 900 and 2000 nm. Several atomic lines are present in this spectral range and indicated directly on the figures. Argon lines are indicated in blue, oxygen in red and carbon in black. Most of these lines are well resolved and separated from one another. Figure 11 shows the OES measurements between 2000 and 2600 nm were CO is observed to emit beginning at 2300 nm. Figure 12 show the 2500 to 4100 nm spectral range, where CO_2 emits from 2650 to 3200 nm. Once again, we can see the partial absorption coming from H_2O due to the humidity of the air at wavelengths around 2800 nm. Figure **13** show the OES measurements from 4100 to 5600 nm. Both CO and CO_2 are present and overlap in this region. CO_2 strongly emits from 4170 to 5000 nm, with the CO_2 headband visible at 4170.5 nm, whereas CO emits from 4294 to 5600 nm. Cold CO_2 presents in the optical path strongly absorbs the signal from 4200 to 4350 nm, even with 90% of the path purged with N_2.

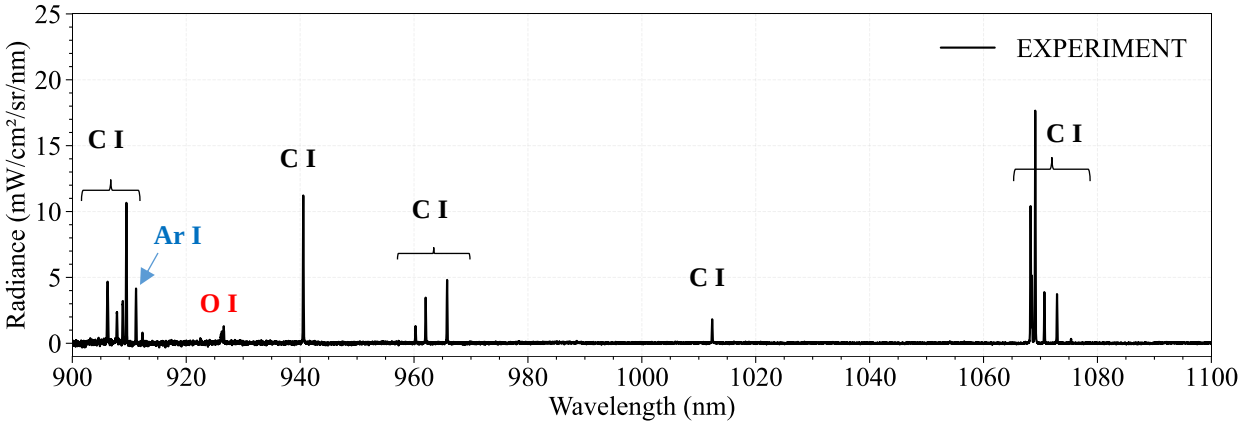

Figure 8. OES measurements between 900 and 1100 nm. Argon lines are indicated in blue, oxygen in red and carbon in black.

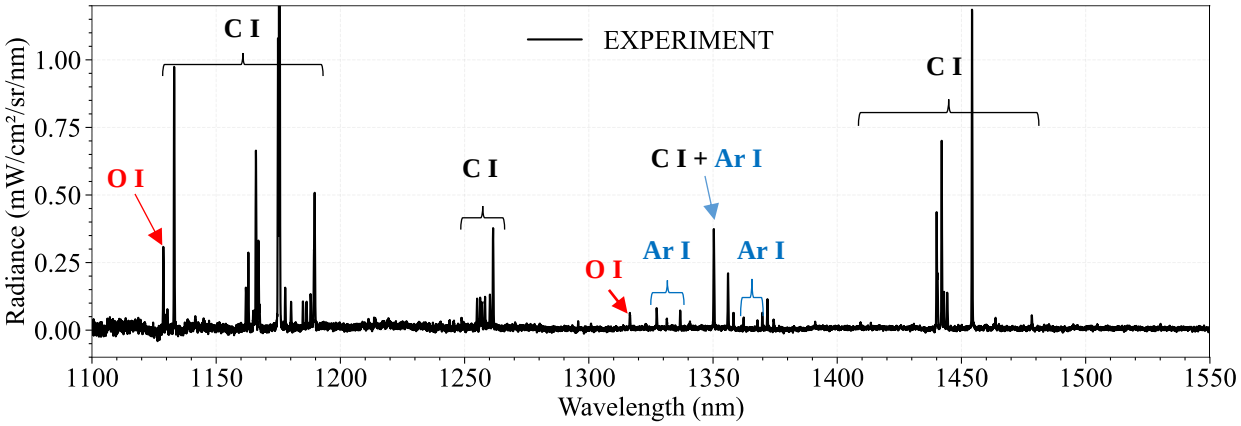

Figure 9. OES measurements between 1100 and 1550 nm. Argon lines are indicated in blue, oxygen in red and carbon in black.

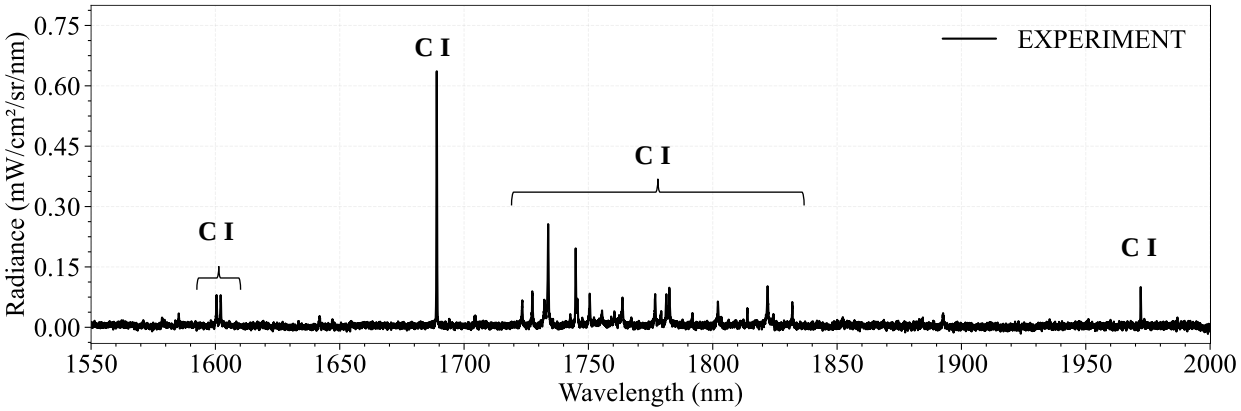

Figure 10. OES measurements between 1550 and 2000 nm. Carbon lines are indicated black.

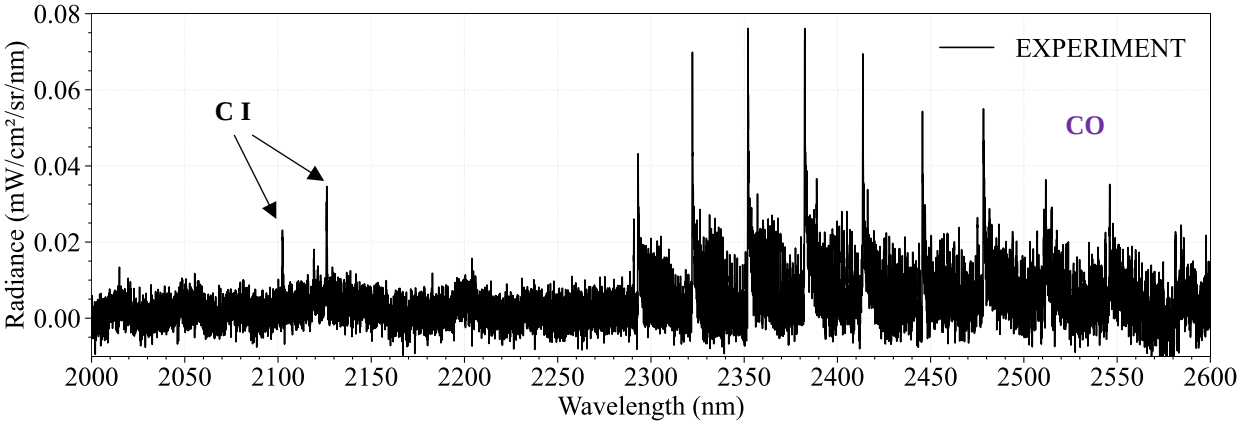

Figure 11. OES measurements between 2000 and 2600 nm. Carbon lines are indicated black. CO is observed to emit beginning at 2300 nm.

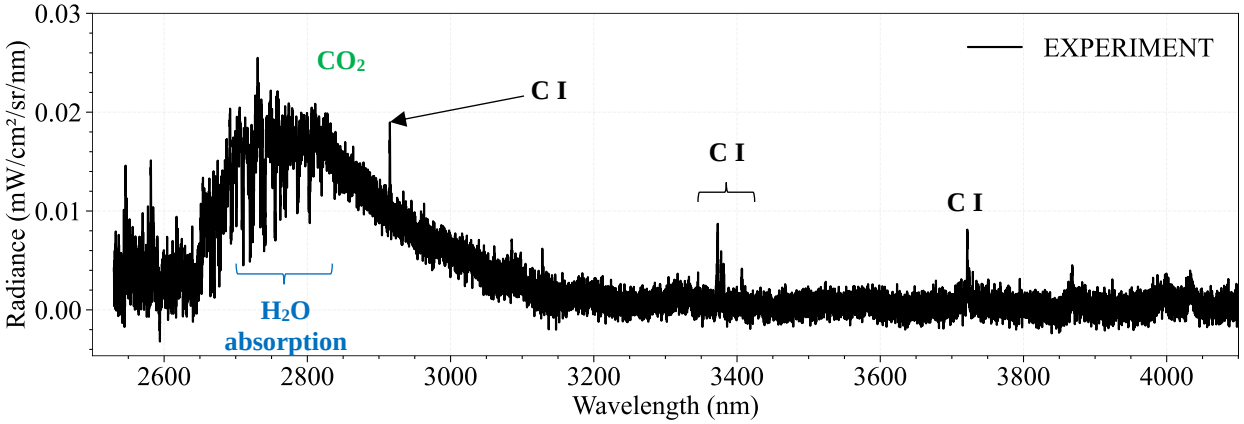

Figure 12. OES measurements between 2500 and 4100 nm. Carbon lines are indicated black. CO_2 emits from 2650 to 3200 nm and is partially absorbed by H_2O due to the humidity of the air around 2800 nm.

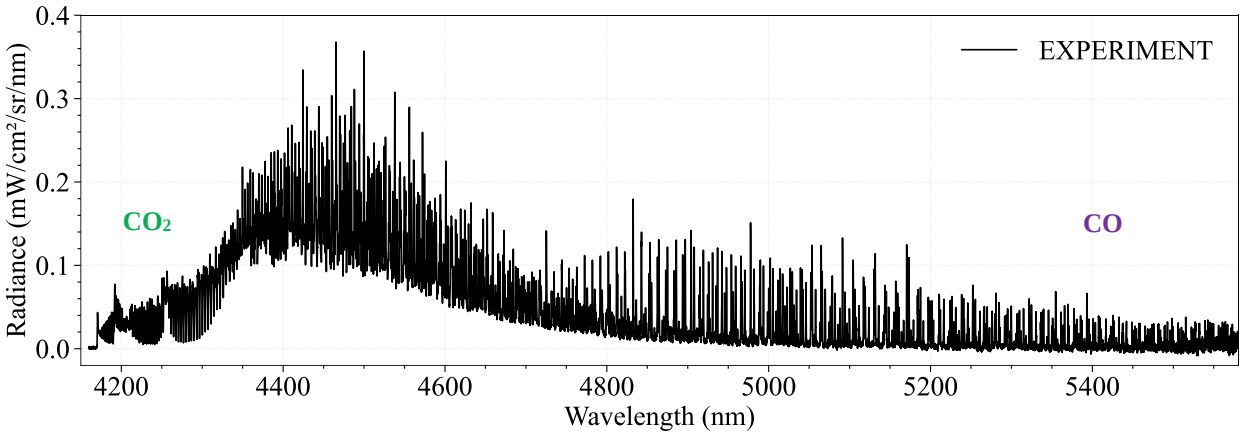

Figure 13. OES measurements between 4100 and 5600 nm. CO_2 strongly emits from 4170 to 5000 nm whereas CO emits from 4294 to 5600 nm. Cold CO_2 presents in the room absorbs the signal from 4200 to 4350 nm.

V. Temperature Analysis

For a plasma in Local Thermodynamic Equilibrium (LTE), the integrated intensity I of a spectral line between an excited electronic level u and a lower level l is related to the LTE temperature T_{LTE} and the pressure P by:

$$\mathbf{I = \frac{A_{ul}}{4\pi}(\varepsilon_u - \varepsilon_l)X_s(T_{LTE})\frac{P}{kT_{LTE}}\frac{g_u}{Q_{el}(T_{LTE})}\exp\left(-\frac{\varepsilon_u}{kT_{LTE}}\right)}$$

where A_{ul} is the Einstein coefficient, g_u is the degeneracy of the upper level and ε_u and ε_l the upper and lower energies. Q_{el} and X_s are respectively the electronic partition function and the mole fraction of the atom `s'[10]. In this equation, the two major sources of uncertainty are the Signal-to-Noise Ratio (SNR) of the experimental measurements (also impacted by the uncertainty of the calibration) and the accuracy of the Einstein coefficients. Depending on the spectral line, these Einstein coefficient accuracies vary from 3% to 10%. The uncertainty on the mole fraction of the atom is impacted by the accuracy of the flowmeters and remains less than 3% over the observed temperature range. The uncertainty on the pressure is estimated at less than 2%. The combined uncertainty on the temperature measurements remains less than 3% at the center of the plasma. The radial temperature profiles presented in Figure 14 were obtained by measuring the absolute intensity of several atomic lines listed in Table 2. These intensities are Abel-inverted to obtain their radially resolved emission. The NASA CEA code [16] was used to determine the equilibrium mole fractions of the gas mixture as a function of temperature. Then using the constants associated with each atomic line

and the operating conditions, the intensity of the measured lines is calculated as a function of temperature and compared with the measurements in order to have the LTE temperature. The complete procedure is detailed in [10].

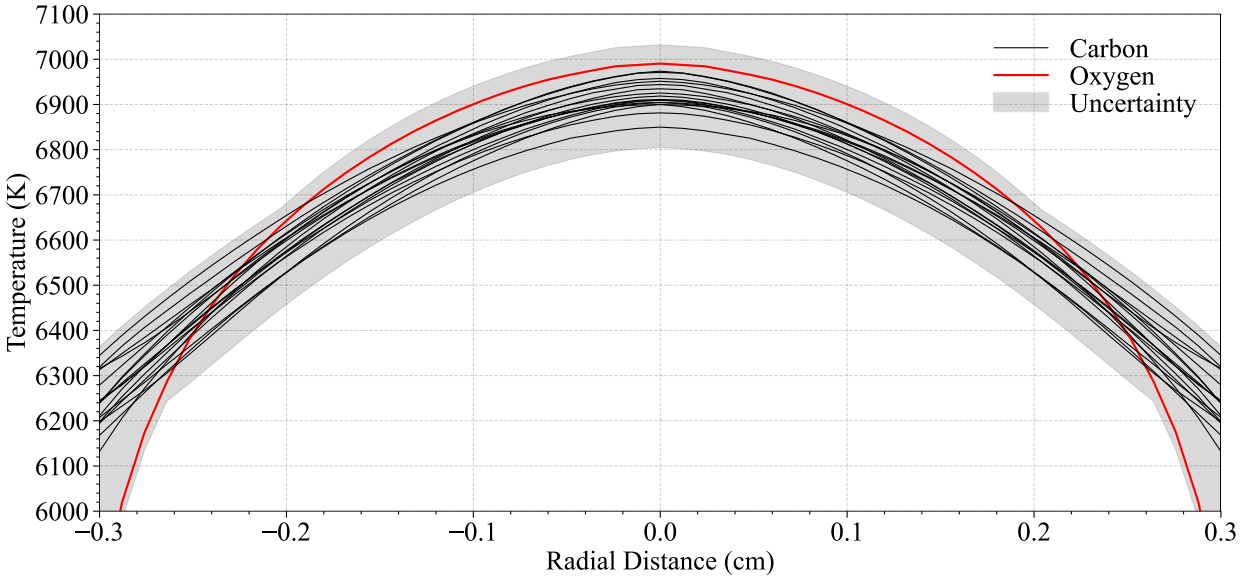

Figure 14. Temperature measurements using carbon (black) and oxygen (red) atomic lines. The associated uncertainty is presented in gray.

As show Figure 14, the centerline temperatures obtained from various atomic features are all equal to within their uncertainty and yield a temperature of 6920±100K. Beginning at approximately 0.25 cm radial distance (half of the radius of the plasma), the temperature from the oxygen 926 nm lines begins to differ from the other temperature estimates, this is due to the low SNR on this line. This method gives the temperature quite accurately within the central hot portion of the plasma jet. However, in the colder regions of the jet beyond a radius of 0.3 cm, the atomic lines do not radiate sufficiently to provide a measure of temperature. For the OES measurements that follow, the average temperature provided by all atomic lines is used at a given radial distance to compute a spectrum for comparison.

Table 2 Atomic lines used for the temperature measurement taken from NIST database

Atom	Observed wavelength air λ (nm)	Accuracy (%)	Energy level ε_u (cm^{-1})
C I	906.14 - 906.25	10	71385 - 71365
C I	909.48	10	71385
C I	911.18	10	71365
O I	926.08 - 926.6	3	97421
C I	940.57	7	72611
C I	962.08	10	70744
C I	965.84	10	70744
C I	1068.31 - 1069.12	10	69689 - 69744
C I	1070.73	10	69689
C I	1072.95	10	69711
C I	1133.03	10	77680
C I	1174.82 - 1175.48	10	78199 - 78216
C I	1189.29 - 1189.58	10	78117 - 78148
C I	1261.41	10	79311
C I	1133.03	10	77680
C I	1439.97 - 1440.33	10	78308 - 78294
C I	1454.25	10	68856
C I	1689.04	10	78530

VI. Comparison with SPECAIR code

As mentioned before, the temperature in the colder regions of the jet, after 0.3 cm remain unknown. This is problematic for the simulation of the emission coming from CO_2 (and to a lesser extent for the "cold" CO lines emitted below 5200 nm) as the major contribution for these bands is coming from the colder region between 2000 and 3000 K. Figure 15 shows the radial profile of the CO_2 headband emission observed at 4170.5 nm. This profile corresponds to the line-of-sight radiance as a function of lateral position (i.e. it is not Abel-inverted). We can clearly see that the maximum emission is reached at 0.4 cm, where we have no information concerning the temperature of the plasma from the atomic temperature measurements. Therefore, we will not compare our experiment to simulations over the spectral range 2600 – 5200 nm in this paper. We are currently working to use the emission from CO_2 to measure the temperature of the jet in these cold boundary regions. Note that the asymmetry observed in this profile is only observed for species emitting at relatively low temperature (2000 3000 K) and is not observed in the spectra coming only from the hotter portions of the jet. The atomic lines or the portions of the CO molecular band above 5200 nm are observed to have profiles that are quite symmetric about the jet centerline.

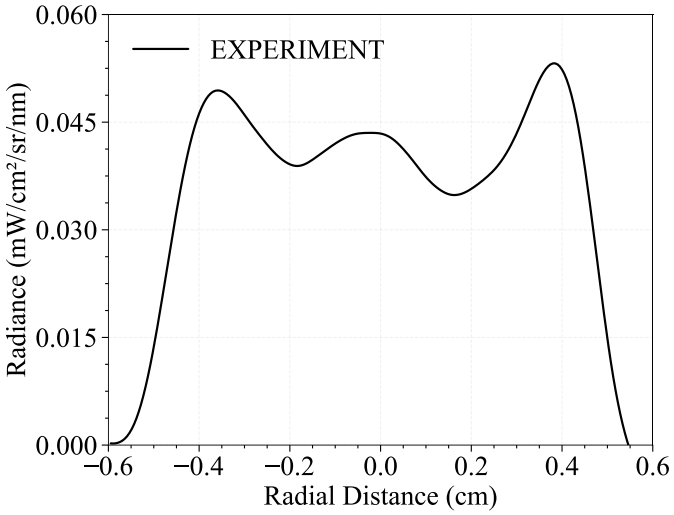

Figure 15. CO_2 headband radial profile at 4170.5 nm.

A. Wavelength Range: 900 – 2000 nm

Figure 16 to Figure 19 show the comparison between the OES measurements and the SPECAIR predictions between 900 and 2000 nm. Several carbon lines are missing in the SPECAIR code, but the for the ones implemented, their intensities are close to the experiment and lie within the uncertainty bounds. The latest version of the NIST database will be implemented into SPECAIR in future work. The following figures show the agreement between our experiment and SPECAIR for the centerline LOS emission, similar agreements are observed for other radial positions down to 0.3 cm.

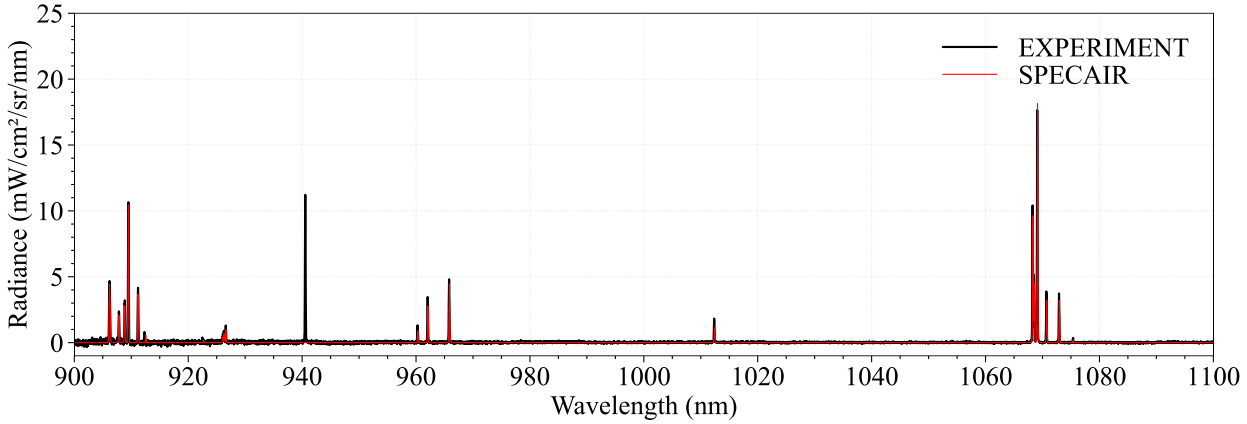

Figure 16. Comparison between experimental spectrum and SPECAIR prediction between 900 and 1100 nm.

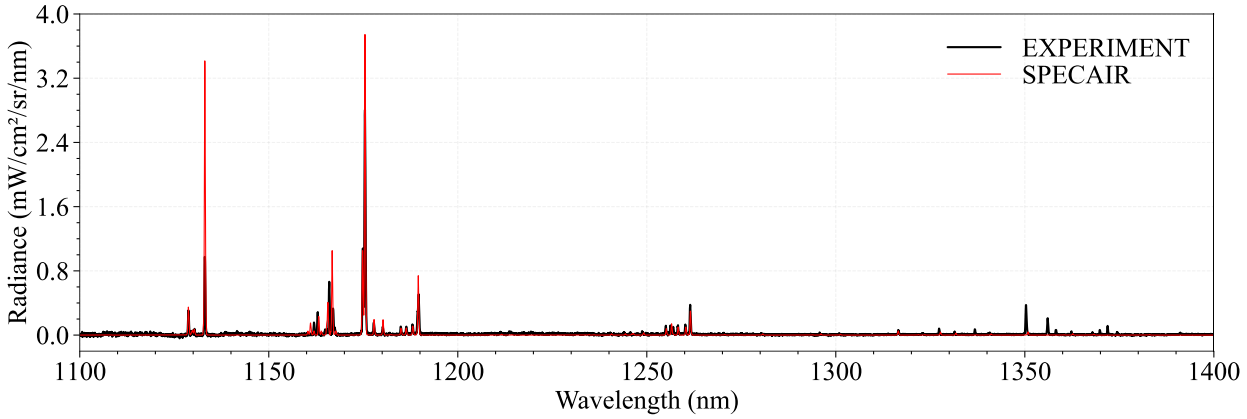

Figure 17. Comparison between experimental spectrum and SPECAIR prediction between 1100 and 1400 nm.

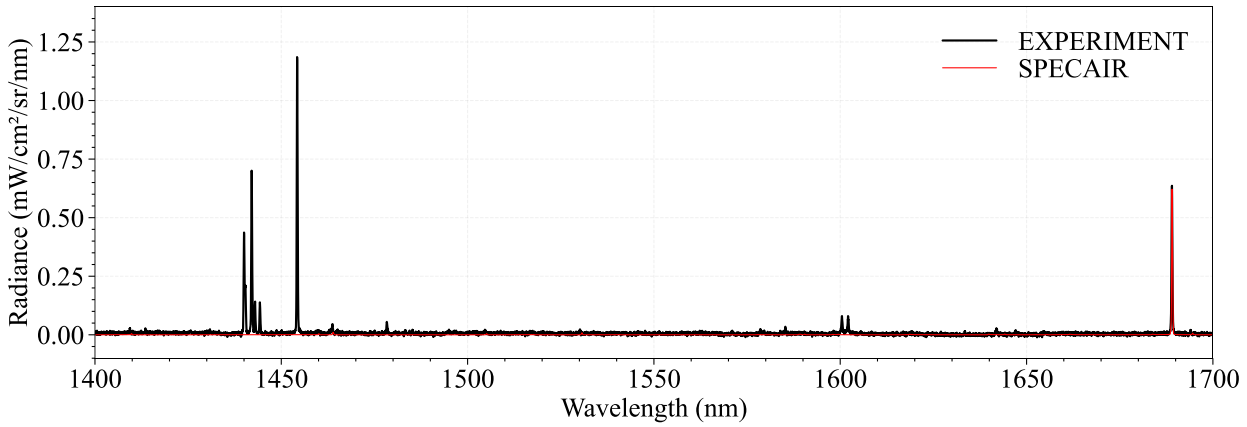

Figure 18. Comparison between experimental spectrum and SPECAIR prediction between 1400 and 1700 nm.

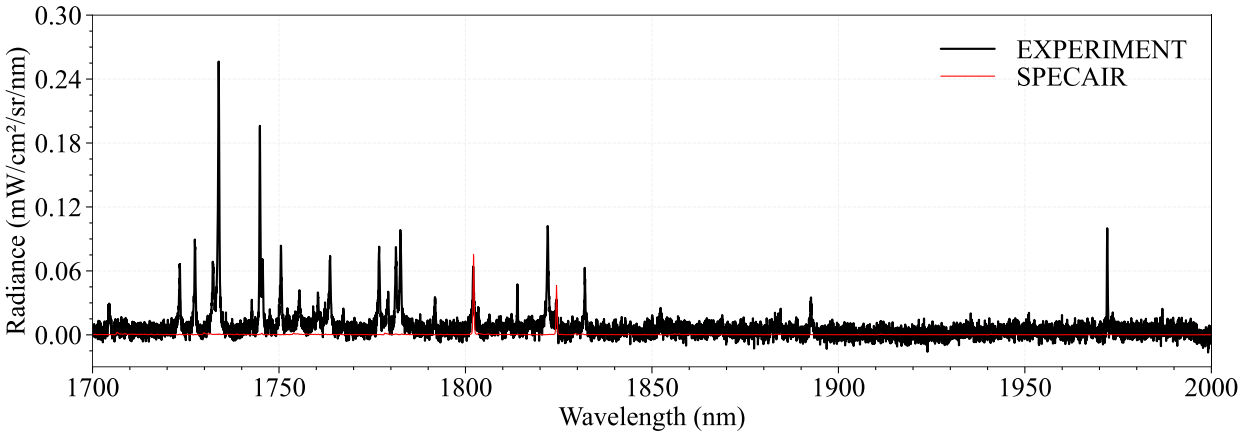

Figure 19. Comparison between experimental spectrum and SPECAIR prediction between 1700 and 2000 nm.

B. Wavelength Range: 2275 – 2600 nm and 5200 – 5600 nm

Figure 20 and Figure 21 show the comparison between our OES measurements and SPECAIR for the CO molecular bands between 2275 and 2600 nm and 5200 and 5600 nm. The agreement between our experiment and SPECAIR over these regions is satisfying as the structure and the absolute intensity are well matched. Future work will include Herman-Wallis correction factors for the rotational line intensities.

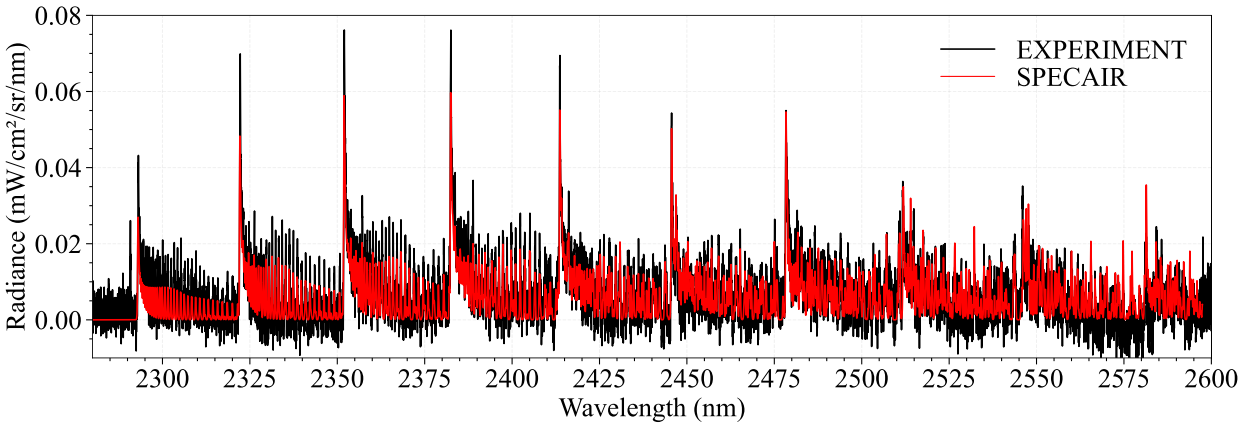

Figure 20. Comparison between experimental spectrum and SPECAIR prediction between 2275 and 2600 nm for the CO molecular band.

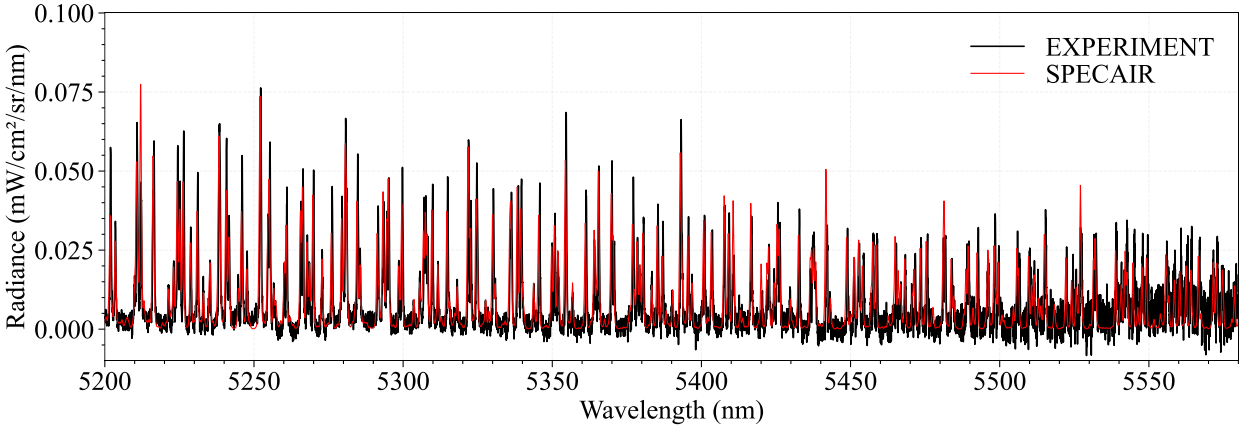

Figure 21. Comparison between experimental spectrum and SPECAIR prediction between 5200 and 5600 nm for the CO molecular band.

VII. VII. Conclusion and Future work

We presented optical emission spectroscopy measurements from a CO_2/Ar plasma jet at 6920 K under equilibrium conditions. The absorption from room air was computed and integrated in the calibration procedure to provide comparison between measured spectra calibrated in absolute intensities and the prediction from the radiation code SPECAIR. Overall a good agreement was observed, highlighting the equilibrium conditions of the plasma and the robustness of our calibration procedure. The same procedure will be used in the future for different plasma conditions.

Future work will focus on estimating or measuring the temperature at the edges of the plasma by using the RADIS code to analyze the CO_2 molecular bands between 2.6 and 3.2 µm and between 4.1 and 5.0 µm [13]. The RADIS code will use the CDSD-4000 database for this analysis [17]. It is hoped that the combination of CO_2 temperature measurements at the boundary with the temperature measurements presented in this paper will enable us to have a full temperature profile across the plasma jet. We will then apply these same measurements to the recombination setup presented in Refs.[6], [7], which uses a water-cooled tube to force plasma cooling and recombination. Temperature and OES measurements will be made at different water-cooled tube lengths between 5 and 30 cm to observe what happens as the plasma is continually cooled. Our calibration procedure, detailed in this paper and validated at the exit of the torch, will be used. Our goal is to track the thermochemical state of the plasma and, in particular, to see if the plasma remains close to LTE conditions or departs from equilibrium as has been previously observed for N_2/Ar mixtures studied using this configuration [6], [7]. To complete this dataset, power balance measurements will also be performed. For these, the water temperatures at the inlet and outlet of the water-cooled tube are measured and used to calculate the enthalpy removed from the plasma. This drop-in enthalpy can then be compared with estimates based upon the thermochemical state of the plasma at the inlet and exit of the water-cooled tube as a consistency check.

Acknowledgments

This work was financially supported by the CO2REC grant (Number: ANR-18-CE05-0003) from the Agence Nationale de la Recherche (ANR).

References

[1] I. Cozmuta, M. J. Wright, B. Laub, and W. H. Willcockson, "Defining ablative thermal protection system margins for planetary entry vehicles," *42nd AIAA Thermophys. Conf.*, no. June, pp. 1–27, 2011.

[2] Dr. David R. Williams, "Mars Fact Sheet," 2018. [Online]. Available: https://nssdc.gsfc.nasa.gov/planetary/factsheet/marsfact.html. [Accessed: 01-Oct-2019].

[3] C. O. Johnston, A. M. Brandis, and K. Sutton, "Shock layer radiation modeling and uncertainty for mars entry," *43rd*

AIAA Thermophys. Conf. 2012, no. June, pp. 1–43, 2012.
[4] C. O. Johnston and M. Panesi, "Advancements in afterbody radiative heating simulations for earth entry," *46th AIAA Thermophys. Conf.*, no. June, pp. 1–19, 2016.
[5] J. Annaloro, A. Bultel, and P. Omaly, "Detailed kinetic of CO2 dissociation and C ionization: Application to atmospheric Martian entries," *J. Phys. Conf. Ser.*, vol. 511, no. 1, 2014.
[6] C. O. Laux, L. Pierrot, and R. J. Gessman, "State-to-state modeling of a recombining nitrogen plasma experiment," *Chem. Phys.*, vol. 398, no. 1, pp. 46–55, 2012.
[7] A. Tibère-Inglesse, S. McGuire, and C. O. Laux, "Nonequilibrium radiation from a recombining nitrogen plasma," *AIAA Aerosp. Sci. Meet. 2018*, no. 210059, 2018.
[8] S. D. McGuire, A. C. Tibère-Inglesse, and C. O. Laux, "Infrared spectroscopic measurements of carbon monoxide within a high temperature ablative boundary layer," *J. Phys. D. Appl. Phys.*, vol. 49, no. 48, 2016.
[9] C. Grimaldi, S. McGuire, A. C. Tibère-Inglesse, and C. O. Laux, "Temperature and radiation measurements of an atmospheric pressure CO 2 plasma," pp. 1–9, 2020.
[10] C. O. Laux, T. G. Spence, C. H. Kruger, and R. N. Zare, "Optical diagnostics of atmospheric pressure air plasmas---Stanford University.pdf," vol. 12, pp. 125–138, 2003.
[11] M. E. MacDonald, C. M. Jacobs, C. O. Laux, F. Zander, and R. G. Morgan, "Measurements of air plasma/ablator interactions in an inductively coupled plasma torch," *J. Thermophys. Heat Transf.*, vol. 29, no. 1, pp. 12–23, 2015.
[12] "EXPERIMENTAL STUDY AND MODELING OF INFRARED AIR PLASMA RADIATION Christophe O. Laux, * Richard J. Gessman, ** Benoît Hilbert, † and Charles H. Kruger ‡ High Temperature Gasdynamics Laboratory – Mechanical Engineering Department Stanford University – Stanf," 1995.
[13] E. Pannier and C. O. Laux, "RADIS: A nonequilibrium line-by-line radiative code for CO2 and HITRAN-like database species," *J. Quant. Spectrosc. Radiat. Transf.*, vol. 222–223, pp. 12–25, 2019.
[14] L. S. Rothman *et al.*, "HITEMP, the high-temperature molecular spectroscopic database," *J. Quant. Spectrosc. Radiat. Transf.*, vol. 111, no. 15, pp. 2139–2150, 2010.
[15] D. Packan, C. O. Laux, R. J. Gessman, L. Pierrot, and C. H. Kruger, "Measurement and modeling of OH, NO, and CO2 infrared radiation at 3400 K," *J. Thermophys. Heat Transf.*, vol. 17, no. 4, pp. 450–456, 2003.
[16] B. J. McBride, *Computer Program for Calculation of Complex Chemical Equilibrium Compositions and Applications*. NASA, 1996.
[17] S. A. Tashkun and V. I. Perevalov, "CDSD-4000: High-resolution, high-temperature carbon dioxide spectroscopic databank," *J. Quant. Spectrosc. Radiat. Transf.*, vol. 112, no. 9, pp. 1403–1410, 2011.